



Pang, W., Gamlath, C., & Cryan, M. (2018). An Optically Controlled Co-Planar Waveguide Millimeter-Wave Switch. *IEEE Microwave and Wireless Components Letters*, 28(8), 669-671.
<https://doi.org/10.1109/LMWC.2018.2840966>

Peer reviewed version

License (if available):
Other

Link to published version (if available):
[10.1109/LMWC.2018.2840966](https://doi.org/10.1109/LMWC.2018.2840966)

[Link to publication record in Explore Bristol Research](#)
PDF-document

This is the author accepted manuscript (AAM). The final published version (version of record) is available online via IEEE at <https://ieeexplore.ieee.org/document/8384021> . Please refer to any applicable terms of use of the publisher.

University of Bristol - Explore Bristol Research

General rights

This document is made available in accordance with publisher policies. Please cite only the published version using the reference above. Full terms of use are available:
<http://www.bristol.ac.uk/red/research-policy/pure/user-guides/ebr-terms/>

An Optically Controlled Co-Planar Waveguide Millimetre Wave Switch

A.W. Pang, C.D. Gamlath, and M.J. Cryan

Department of Electrical and Electronic Engineering, University of Bristol, Bristol, BS8 1TR, U.K.

alex.pang@bristol.ac.uk, m.cryan@bristol.ac.uk

Abstract—This paper demonstrates an optically controlled Co-Planar Waveguide (CPW) switch operating in the millimetre wave region. Full wave electromagnetic analysis used a multi-layer model to simulate the photoinduced plasmas and good agreement between measured and simulated results has been achieved. The insertion loss is less than 4dB and isolation is greater than 15dB from 32GHz-50GHz. This approach requires the use of 175mW of optical power at a wavelength 980nm, but it removes the need for bandwidth limiting electrical bias networks.

Index Terms—Optically induced plasmas (OIP), Co-Planar Waveguide (CPW), millimeter wave (mmW), optical switch

I. INTRODUCTION

Reconfigurable Radio Frequency (RF), microwave and millimetre wave (mmW) switches are an important aspect of most communication systems [1]. The unprecedented challenge of accommodating multiple wireless standards has encouraged the development of tunable RF circuits and switches. Reconfigurable circuitry reduces system size and removes the requirement for duplicating the same circuits, thus reducing system cost. Currently, reconfigurable circuits are typically based on varactors, PIN diodes, transistors or RF MicroElectroMechanical Systems (RF MEMS) [2-6]. Varactors and PIN diodes have low insertion loss and continuous frequency band tuning but power handling problems can affect their performance and since they are diodes give poor non-linear performance [2-6]. RF MEMS switches provide excellent isolation values and linear behaviour and mmW examples have been shown recently [7]. However, issues with reliability occur when handling high power signals, in particular with “hot-switching” [8-12]. A major issue for all these approaches is the requirement for DC bias lines. At millimetre wave frequencies and above, this can lead to complex bias circuits and parasitic effects which can degrade their performance.

Therefore, there is a requirement for alternative technologies that work well at these very high frequencies. One such approach is based on Optically Induced Plasmas (OIPs) [13-17]. Our previous work has described the basic physics of a microstrip gap based optical switch [18]. Here a microstrip gap is defined on a silicon substrate and the gap is illuminated by light with energy above the band gap of the semiconductor. In this case a plasma region made up of electron and hole pairs is created and this area becomes electrically conductive. We have developed several such switches and switchable antennas based on microstrip lines and patch antennas [18-20], however microstrip tends not to perform well at millimetre wave frequencies. In particular, CPW reduces surface waves modes and hence reduces dispersion and radiative losses [21]. Thus, here we explore the use of Co-Planar Waveguide (CPW) as the

transmission line, not only does this give good high frequency performance, the switch topology becomes more flexible since the centre conductor can now be grounded easily resulting in a normally-ON type switch. Previously, a silicon substrate CPW switch has been demonstrated in [16] with good insertion loss and isolation values up to 25GHz. However, [16] is a silicon integrated circuit approach, whereas this paper shows a hybrid integrated approach with a silicon superstrate that could be easily incorporated into large complex circuits. OIP based switches have been shown to have very good linearity at high power levels, such as input power of 30dBm in [13], and this hybrid integration approach is more suitable for high power applications. Our approach also uses backside illumination which allows for simple integration and heat sinking of the light source. Hybrid integration has also been shown in [15] up to 7GHz, but here we perform detailed 3D electromagnetic modelling and show good measured switching performance to 50GHz. In general, the main shortcoming of optically controlled switches is the DC power requirement for the light source. However, applications such as Radar and wireless communication basestations, which already have large power consumption and may not be affected by an additional 1-2W in the power budget. There are also new light source technologies such as microLEDs which have high optical intensities and can be easily integrated with our approach [22].

This paper will firstly introduce the Grounded CPW design based on a fused silica glass substrate which allows for back side illumination. Then a model is developed using Finite Integration in Time based CST simulation which describes the plasma region as a series of conductive layers. V-connector based measurements are compared with the modelled results and good agreement is shown.

II. FABRICATION AND MEASUREMENT SETUP

An important feature of this work is the use of optically transparent fused silica glass ($\epsilon_r=3.5$) as a low loss microwave substrate. This allows bottom side illumination which produces a highly-integrated device. The fused silica substrate is 500 μ m thick and was lithographically processed to create gold CPW transmission lines. Fig. 1 shows the top view of the Grounded Co-Planar Waveguide (GCPW) circuit sample covered by a silicon superstrate and mounted on a brass block fixture. The central line width (w) is 0.6mm and spacing (s) between the central line and the grounding planes is 0.08mm.

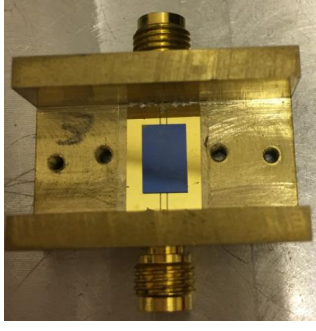


Fig.1. Top view of GCPW circuit sample with line width (w) 0.6mm and spacing (s) 0.08mm

Fig. 2(a) shows a top view of the switch with two illumination regions in the spacing of the CPW such that when illuminated from below the low resistance of the plasma regions short circuit the CPW line. A piece of silicon, 8mm x 5mm x 0.5mm ($\epsilon_r=11.9$) is used as a superstrate which is placed over the GCPW. The silicon superstrate was a lightly doped n-type wafer with $\langle 100 \rangle$ orientation and resistivity $> 10 \text{ k}\Omega \cdot \text{cm}$. The silicon has a 300nm thick passivated layer of silicon dioxide to prevent a Schottky contact forming at the metal and semiconductor interface. Fig. 2(b) shows the schematic end view of the test fixture demonstrating how the light source is integrated into the system. Optical illumination is provided by a 980nm wavelength fibre coupled laser diode (Roithner Lasertechnik). This was chosen due to the high carrier generation efficiency at this wavelength. The fibre laser is coupled through a hole in the brass block which has been designed to have minimal effect on the millimetre wave response. In this case the majority of the laser power is not being used to illuminate the silicon due to the nature of the CPW gaps.

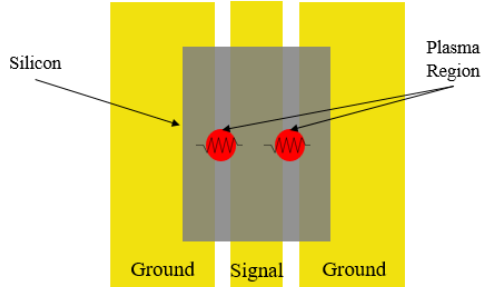


Fig. 2(a). Top view of optically controlled GCPW switch layout

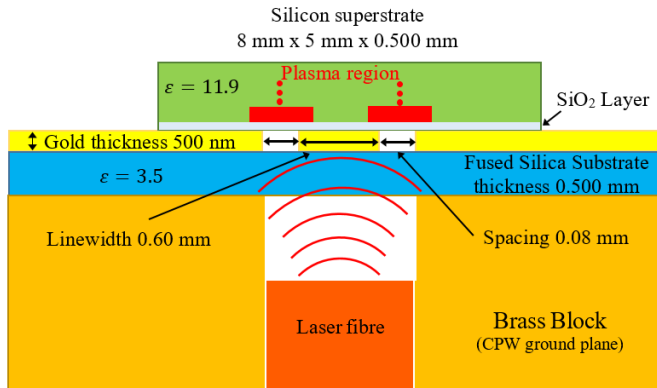


Fig. 2(b). Schematic end view of optically controlled GCPW switch with bottom illumination

III. SIMULATION AND MEASUREMENT

CST is used as a full wave 3D Electromagnetic modelling tool [23]. The plasma region can be represented by a series of varying conductivity layers as described in [18] and Fig. 3 shows the conductivity profile used in this work.

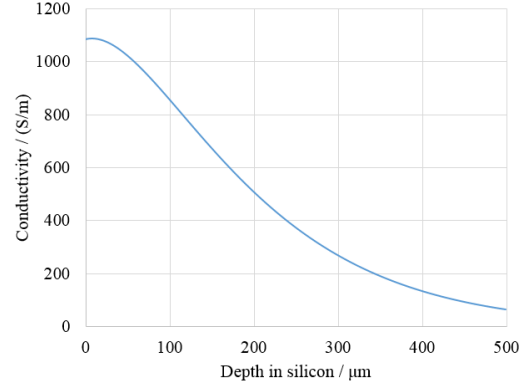


Fig. 3. Conductivity vs. diffusion depth in silicon superstrate

The corresponding parameters are taken as absorption depth = $96\mu\text{m}$ [24], bulk recombination time = $10\mu\text{s}$, diffusion length = $120\mu\text{m}$ [18]. Illumination power of 175 mW corresponding to 1100 S/m conductivity at plasma surface layer has been used in the measurement and CST simulation respectively. Fig. 4 shows the ten cascaded conductive layers derived from Fig. 3. There are two plasma regions, and each one is $1200\mu\text{m} \times 480\mu\text{m}$ in area and $480\mu\text{m}$ high. The size of these is chosen to represent (i) the illumination spot size, (ii) the effects of sideways carrier diffusion, and (iii) the vertical exponential decay taken from Fig. 3. In future work 3D exponentially decaying plasma regions will be used which will more closely represent the real carrier distributions. In addition, a gap has been left between the gold layer and the bottom conductive layer of $20\mu\text{m}$ to simulate the metal-insulator-plasma contact transition and obtain good agreement at low frequencies.

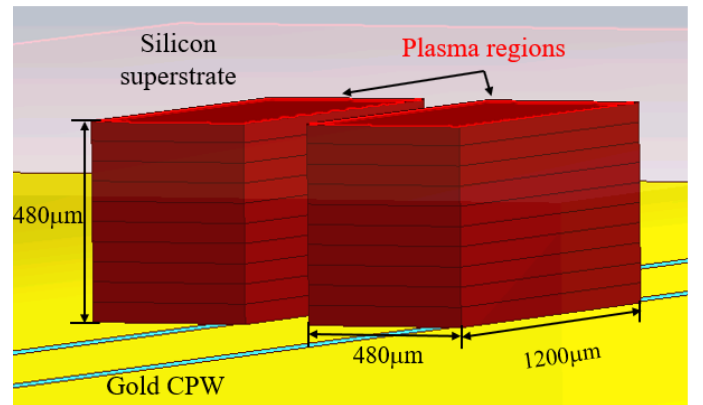


Fig. 4. Plasma layers within silicon superstrate in CST view

Fig. 5 shows the CST simulated and Vector Network Analyser (VNA) measured S_{21} of the GCPW in the ON and OFF conditions. It can be seen that good overall agreement has been obtained. With no laser illumination, this switch has reasonably good insertion loss with less than 4dB through the frequency band of DC to 50GHz. When illumination is provided, a conductive path is created between the central track and the ground planes of the GCPW. This low resistance increases the

insertion loss to more than 15dB above 32GHz and a large dip at 46.5GHz of 28.7dB. The resonant dips around 33GHz and 39GHz may be associated with bulk mmW resonances in the silicon and further work is being carried out to confirm this. An important aspect of these results is that the CPW spacing defines the plasma illumination area and hence the resistance to ground. In this case since there is a thin insulating layer between the silicon and the gold, these DC effects are masked. Figure 6 shows CST simulated results for three different CPW spacings. It can be seen that only very small differences occur in these cases.

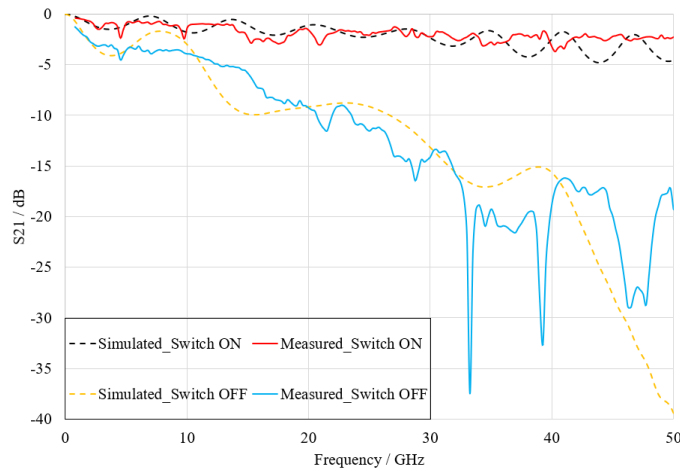


Fig. 5. Measured and Simulated S_{21} of GCPW with linewidth, $w=0.6\text{mm}$ and spacing, $s=0.08\text{mm}$ at Switch ON/OFF conditions

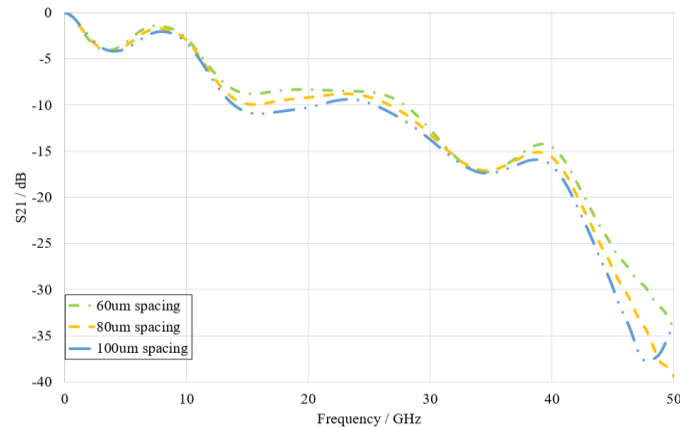


Fig. 6. Simulated S_{21} of GCPW with linewidth, $w=0.6\text{mm}$ and varying spacing values at Switch ON condition

IV. CONCLUSION

This paper reports a bottom illuminated optically controlled millimetre wave GCPW switch with low insertion loss up to 50 GHz and an off-state isolation greater than 15dB from 32GHz to 50GHz. Good agreement with electromagnetic modelling has been shown. It is believed that optimisation of the GCPW geometry to more efficiently use the available optical power, modification of circuit grounding and laser coupling will further improve the switch performance. Optically induced plasmas are inherently frequency independent in nature and thus it is envisaged that the performance of such devices will be equally good in even higher frequency ranges. This is particularly encouraging since conventional switching approaches become

much more difficult to implement in these higher frequency ranges.

REFERENCES

- [1] R. Berezdivin, R. Breinig, and R. Topp, "Next-Generation Wireless Communications Concepts and Technologies," *IEEE Commun. Mag.*, vol. 40, no. 3, pp. 108-116, Mar. 2002.
- [2] C. G. Christodoulou *et al.*, "Reconfigurable antennas for wireless and space applications," *Proc. IEEE*, vol. 100, no. 7, pp. 2250-2261, Jul. 2012.
- [3] N. Behdad and K. Sarabandi, "Varactor-tuned dual-band slot antenna," *IEEE Trans. Antennas Propag.*, vol. 54, no. 2, pp. 401-408, Feb. 2006.
- [4] S.-J. Wu and T.-G. Ma, "A wideband slotted bow-tie antenna with reconfigurable CPW-to slotline transition for pattern diversity," *IEEE Trans. Antennas Propag.*, vol. 56, no. 2, pp. 327-334, Feb. 2008.
- [5] J.G. Yang, and K. Yang, "Ka-band 5-bit MMIC phase shifter using InGaAs PIN switching diodes," *IEEE Microw. Wireless Compon. Lett.*, vol. 21, no.3, pp.151-153, Mar. 2011.
- [6] T., Boles *et al.*, "AlGaAs PIN diode multi-octave, mmW switches," *In Microwaves, Communications, Antennas and Electronics Systems (COMCAS)*, IEEE International Conference, 2011, pp. 1-5.
- [7] Riazat M, Majidi-Ahy R, Feng JI. Propagation modes and dispersion characteristics of coplanar waveguides. *IEEE transactions on microwave theory and techniques*. 1990 Mar;38(3):245-51.
- [8] G. M. Rebeiz, and J. B. Muldavin, "RF MEMS switches and switch circuits," *IEEE Microwave magazine*, vol. 2, no. 4, pp. 59-71, Dec. 2011.
- [9] C. D. Patel, and G. M. Rebeiz, "A high-reliability high-linearity high-power RF MEMS metal-contact switch for DC-40-GHz applications," *IEEE Trans Microw. Theory Tech.* vol. 60 no.10, pp. 3096-3112, Oct. 2012.
- [10] L. L. W. Chow *et al.*, "Lifetime Extension of RF MEMS Direct Contact Switches in Hot Switching Operations by Ball Grid Array Dimple Design," *IEEE Electron Device Letters*, vol. 28, no. 6, pp. 479-481, June 2007.
- [11] J.B. Muldavin, and G. M. Rebeiz, "High-isolation CPW MEMS shunt switches. 1. Modeling," *IEEE Trans. Microw. Theory Tech.*, vol. 48, no. 6, pp. 1045-1052, Jun. 2000.
- [12] K. Hettak, G. A. Morin, and M. G. Stubbs, "DC-to-50 GHz compensation structure for flip-chip assembled SPST MEMS switch," in *Microwave Symposium Digest, 2009. MTT'09. IEEE MTT-S International*, pp. 597-600.
- [13] T. Kaneko, *et al.*, "Microwave switch: LAMPS (light activated microwave photoconductive switch)," *IEEE Electron. Lett.*, vol. 39, no. 12, pp. 917-919, Jun. 2013.
- [14] C. J. Panagamuwa, A. Chauraya, and J. C. Vardaxoglou, "Frequency and beam reconfigurable antenna using photoconducting switches," *IEEE Trans. Antennas and Propag.*, vol. 54, no. 2, pp. 449-454, Feb. 2006.
- [15] J.R. Flemish, and R. L. Haupt, "Optimization of a photonic controlled microwave switch and attenuator," *IEEE Trans. Microw. Theory Tech.*, vol. 58, no. 10, pp. 2582-2588, Oct. 2010.
- [16] K. B. Ali *et al.*, "Photo-Induced Coplanar Waveguide RF Switch and Optical Crosstalk on High-Resistivity Silicon Trap-Rich Passivated Substrate," *IEEE Trans. Electron Devices*, vol. 60, no. 10, pp.3478-3484, Oct. 2013.
- [17] M. Kulygin *et al.*, "Nanosecond Microwave Semiconductor Switches for 258... 266 GHz," *Journal of Infrared, Millimeter, and Terahertz Waves*, vol. 36, no. 9, pp. 845-855, Sep. 2015.
- [18] C. D. Gamlath, D. M. Benton, M. J. Cryan, "Microwave Properties of an Inhomogeneous Optically Illuminated Plasma in a Microstrip Gap," *IEEE Trans. Microw. Theory Tech.*, vol. 63, no. 2, pp. 374-383, Feb. 2015.
- [19] A. W. Pang, S.B. Smida, C. D. Gamlath, and M. J. Cryan, "Non-linear Characteristics of an Optically Reconfigurable Microwave Switch," *IET Microw., Antennas & Propag.*, accepted in Jan. 2018, to be published.
- [20] C. D. Gamlath *et al.*, "Investigation of an optically induced superstrate plasma for tuning microstrip antennas," *IET Optoelectronics*, vol. 11, no. 6, pp. 230-236, Sep. 2017.
- [21] N. Vahabisani, and M. Daneshmand, "Monolithic Millimeter-Wave MEMS Waveguide Switch," *IEEE Trans. Microw. Theory Tech.*, vol. 63, no. 2, pp. 340-351, Feb. 2015.
- [22] A.H. Jeorrett *et al.*, "Optoelectronic tweezers system for single cell manipulation and fluorescence imaging of live immune cells," *Optics express*, vol. 22, no. 2, pp. 1372-1380, Jan. 2014.
- [23] CST Microwave Studio 2016, Computer Simulation Technology, 2016, <https://www.cst.com/>
- [24] M.A. Green, and M. J. Keevers, "Optical properties of intrinsic silicon at 300 K", *Progress in Photovoltaics: Research and Applications*, vol. 3, no. 3, pp. 189-192, Jan. 1995.